

Efficient forward modeling for DNAPL site evaluation and remediation

Todd Arbogast & Steven Bryant

*Center for Subsurface Modeling, Texas Institute for Computational and Applied Mathematics, C0200,
The University of Texas at Austin, Austin, Texas 78712, USA.*

ABSTRACT: Although the general characteristics of DNAPL flow and transport in the subsurface are reasonably well understood, it is often difficult and expensive to pinpoint sources of DNAPL contamination. Inversion techniques to improve site characterization rely on a forward model of multiphase flow. Ideally the forward model would be very fast, so that many realizations can be carried out in order to quantify and reduce uncertainty, yet capable of handling large numbers of grid elements, so that more accurate (small scale) determinations of soil properties and DNAPL content can be made. To meet these conflicting requirements of speed and detail in the forward modeling of contamination events, we present a subgrid-scale numerical technique for upscaling multiphase flow. Upscaling is achieved by explicitly decomposing the differential system into a coarse-grid-scale operator coupled to a subgrid-scale operator. The subgrid-scale operator is approximated as an operator localized in space to a coarse-grid element. An influence function (numerical Greens function) technique allows us to solve these subgrid-scale problems independently of the coarse-grid approximation. The coarse-grid problem is modified to take into account the subgrid-scale solution and solved as a large linear system of equations. Finally, the coarse scale solution is corrected on the subgrid-scale, providing a fine-grid scale representation of the solution. In this approach, no explicit macroscopic coefficients nor pseudo-functions result. The method is easily seen to be optimally convergent in the case of a single linear parabolic equation. The method is fast, robust, and achieves good results.

1 INTRODUCTION

We give a preliminary report on the use of a novel upscaling procedure used to discretize the equations of two-phase flow. The idea behind the procedure was first introduced in (Arbogast, Minkoff, & Keenan 1998) for single phase flow. For some recent modifications and two-phase extensions without gravitational effects, see (Arbogast 2000). We apply the technique to systems that possess gravitational and capillary forces, since these dominant DNAPL spill scenarios.

There are a number of ideas that underly the choice of discretization. DNAPL problems require a great deal of computer power and grid resolution for a number of reasons. First, DNAPL saturations tend to be small and we are therefore near the degeneracy in the differential saturation equation. A fine mesh is required to resolve these effects. Second, the equations are highly nonlinear, so they must be resolved to capture the appropriate nonlinear behavior. Third, the problem domain tends to be very large with ill-defined boundaries, and the time interval of interest is often quite long. Fourth, many problems require the

solution at prior times. Forward solution from a guess at the initial state, repeated many times, is required. Finally, the assessment of risk and the characterization of the site require multiple realizations and simulations.

It is thus imperative that we find an efficient forward model. Our approach is to compute over a coarse grid, since then the solution is more easily obtained. However, we cannot neglect the finer subgrid-scale detail in either the model coefficients or the solution itself, as these feed back into the nonlinear terms. Thus we must use some kind of upscaling technique to resolve the fine scale features. We do this by an explicit expansion of the governing equations into fine (subgrid) and coarse pieces. By a judicious choice of finite element spaces, we are able to decompose the operator so that the subgrid-scale problems are small and disjoint. Then it is just a matter of computing the local coupling between the subgrid and coarse scales.

2 DESCRIPTION OF DIFFERENTIAL MODEL

We present here the equations describing the flow of two immiscible, incompressible fluids in a porous

medium, such as DNAPL and water. For phase $j = w, n$ (i.e., wetting and nonwetting), let s_j , \mathbf{u}_j , and p_j be the phase saturations, Darcy velocities, and pressures. Let $s = s_w = 1 - s_n$, ϕ be the porosity, K the absolute permeability, g the gravitational constant, and z the depth. The mobilities are related to the relative permeabilities and fluid viscosities as $\lambda_j(s) = k_{r,j}(s)/\mu_j$ and $\lambda(s) = \lambda_w(s) + \lambda_n(s)$, and $P_c(s) = p_w - p_n$ is the capillary pressure. Conservation of mass of each phase gives the governing equations. After reformulation into a pressure and saturation equation, we obtain the following two equations (see, e.g., (Chavent & Jaffré 1986; Arbogast 1992)).

Pressure equation:

$$\begin{aligned} \nabla \cdot \mathbf{u} &= f \equiv f_w + f_n, \\ \mathbf{u} &= -K\lambda(s)(\nabla p - \rho(s)\nabla z) = \mathbf{u}_w + \mathbf{u}_n, \end{aligned} \quad (1)$$

where f_j is the well term and the global pressure and density are

$$p = p_n - \int_0^s \frac{\lambda_w(\sigma)}{\lambda(\sigma)} P'_c(\sigma) d\sigma$$

and

$$\rho(s) = \frac{\lambda_w(s)}{\lambda(s)} \rho_w + \frac{\lambda_n(s)}{\lambda(s)} \rho_n.$$

Saturation equation:

$$\begin{aligned} \phi \frac{\partial s}{\partial t} + \nabla \cdot \mathbf{u}_w &= f_w(s), \\ \mathbf{u}_w &= -K\nabla q(s) + \gamma(\mathbf{u}, s), \end{aligned} \quad (2)$$

where the ‘‘complementary’’ potential and γ are

$$\begin{aligned} q(s) &= -\int_0^s \frac{\lambda_w(\sigma)\lambda_n(\sigma)}{\lambda(\sigma)} P'_c(\sigma) d\sigma, \\ \gamma(\mathbf{u}, s) &= \frac{\lambda_w(s)}{\lambda(s)} \mathbf{u} - K \frac{\lambda_w(s)\lambda_n(s)}{\lambda(s)} (\rho_n - \rho_w) g \nabla z. \end{aligned}$$

Note that $q'(0) = q'(1) = 0$ (we consider *reduced* saturations, i.e., saturations linearly scaled so that the residual saturations become 0). Thus, if s_w or s_n is near its residual value, the saturation equation is *degenerate*, meaning that the capillary diffusive flux tends to zero. The above formulation has the advantage that, formally, the equation is parabolic even at the residual values. Note also that this equation may be convection dominated, since the total velocity \mathbf{u} may be large, especially in a pump-and-treat type of scenario. On the other hand, if the system experiences only background flow, then the equation will be dominated by flow arising from capillary and gravitational forces, which tend to cause no *net* flow of fluids (i.e., $\mathbf{u} = 0$), so the degenerate diffusion is critical.

The pressure equation is always well behaved, since $\lambda(s)$ is bounded above and below. It is a uniformly elliptic equation for p , but of course elliptic systems are numerically ill-conditioned.

3 DESCRIPTION OF NUMERICAL MODEL

Let $\Delta t > 0$ be the given time step (these can vary from step to step in practice). For a time dependent quantity φ , let φ^n denote its value at the n th time level $t = t_n = n\Delta t$. We use sequential time splitting to separate the two equations in time. That is, for the n th time level, we replace s by s^{n-1} in the pressure equation. Thus, the pressure equation can be solved for p^n and \mathbf{u}^n independently of the saturation equation. In fact, the equation becomes linear. Multiply the equation (1a) by an appropriate test function w and integrate in space; similarly, multiply (1b) by a vector test function \mathbf{v} , integrate, and apply the divergence theorem (i.e., integration by parts) to obtain the following.

Semi-discrete pressure equation:

$$\begin{aligned} \int \nabla \cdot \mathbf{u}^n w dx &= \int f^n w dx, \\ \int (\lambda(s^{n-1})K)^{-1} \mathbf{u}^n \cdot \mathbf{v} dx &= \int p^n \nabla \cdot \mathbf{v} dx + \int \rho(s^{n-1}) \nabla z \cdot \mathbf{v} dx. \end{aligned} \quad (3)$$

For (2a), use a backward Euler time discretization. In place of (2b), introduce $\psi = -\nabla q(s)$ so that $\mathbf{u}_w = K\psi + \gamma$. After multiplication by test functions, integration, and integration by parts, we get the following.

Semi-discrete saturation equation:

$$\begin{aligned} \int \phi \frac{s^n - s^{n-1}}{\Delta t} w dx &+ \int \nabla \cdot (K\psi^n + \gamma(\mathbf{u}^n, s^n)) w dx \\ &= \int f_w^n(s^n) w dx, \\ \int \psi^n \cdot \mathbf{v} dx &= \int q(s^n) \nabla \cdot \mathbf{v} dx. \end{aligned} \quad (4)$$

We separate the solution and the test functions into the coarse and the finer subgrid scales. For the vector variables \mathbf{u} , ψ , or \mathbf{v} we decompose into the two spaces $\mathbf{V}_c \oplus \delta\mathbf{V}$, and for the scalar variables p , s or w we decompose into $W_c \oplus \delta W$. We choose for these four spaces suitable finite element spaces, the coarse spaces are defined over a coarse mesh, and the sub-grid spaces are defined over a refinement of the coarse mesh. Specifically, we decompose

$$\begin{aligned} \mathbf{u} &= \mathbf{u}_c + \delta\mathbf{u}, \\ \psi &= \psi_c + \delta\psi, \\ \mathbf{v} &= \mathbf{v}_c + \delta\mathbf{v}, \\ p &= p_c + \delta p, \\ w &= w_c + \delta w. \end{aligned} \quad (5)$$

Because the saturation equation is parabolic, it turns out that we do *not* need to consider a decomposition of s .

We choose the lowest order Raviart-Thomas space for $\delta\mathbf{V} \times \delta W$ (Raviart & Thomas 1977), such that

there are no vector variable degrees of freedom on the coarse grid. That is, the velocities do *not* cross coarse grid lines (in 2D) or faces (in 3D). Moreover, for consistency, the scalar variable should average zero on a coarse element. This is like assuming that, restricted to a coarse element, $\delta \mathbf{V} \times \delta W$ has homogeneous Neumann boundary conditions. No flow occurs between coarse elements on the fine scale; it occurs only on the coarse scale. This assumption allows us to treat the subgrid-scale problems as independent (up to the connecting coarse scale).

Because the coarse scale provides all flow across coarse grid interfaces, we use a higher order accurate scheme for the coarse scale. The next higher order space of (Brezzi, Douglas, & Marini 1985) in 2D or of (Brezzi, Douglas, Duràn, & Fortin 1987) in 3D provides the smallest space. These spaces are second order accurate for the velocities (and remain first order accurate for the pressures or saturations). Our choice of spaces allows us to control the coarse-scale coupling, and to thereby devise an efficient solution technique.

The choice of the lowest order Raviart-Thomas spaces on the coarse scale does not appear to be sufficient. In the case of single phase flow, this choice gives only a marginal improvement over simply solving the equations over the coarse scale, ignoring the fine scale variation in the permeability K (Arbogast, Minkoff, & Keenan 1998). In the nonlinear two-phase case, we would expect that such marginal improvement would be insignificant.

Separating the pressure equation into coarse and subgrid pieces yields the following set of equations. It happens that both the finite element pressure function and the divergence of the finite element velocity function are piece-wise constant over the mesh. Moreover, $\nabla \cdot \delta \mathbf{v}$ has average zero over a coarse element. Thus terms like $\int \nabla \cdot \mathbf{v}_c \delta w dx$ and $\int \nabla \cdot \delta \mathbf{v} w_c dx$ vanish.

Coarse pressure equation:

$$\begin{aligned} \int \nabla \cdot \mathbf{u}_c^n w_c dx &= \int f^n w_c dx, \\ \int (\lambda(s^{n-1})K)^{-1} (\mathbf{u}_c^n + \delta \mathbf{u}^n) \cdot \mathbf{v}_c dx & \\ &= \int p_c^n \nabla \cdot \mathbf{v}_c dx + \int \rho(s^{n-1}) \nabla z \cdot \mathbf{v}_c dx. \end{aligned} \quad (6)$$

Subgrid (δ) pressure equation: On each coarse element E_c , we have that

$$\begin{aligned} \int_{E_c} \nabla \cdot \delta \mathbf{u}^n \delta w dx &= \int_{E_c} f^n \delta w dx, \\ \int_{E_c} (\lambda(s^{n-1})K)^{-1} (\mathbf{u}_c^n + \delta \mathbf{u}^n) \cdot \delta \mathbf{v} dx & \\ &= \int_{E_c} \delta p^n \nabla \cdot \delta \mathbf{v} dx \\ &+ \int_{E_c} \rho(s^{n-1}) \nabla z \cdot \delta \mathbf{v} dx. \end{aligned} \quad (7)$$

Note that $\delta \mathbf{v}$ and $\delta \mathbf{u}$ do not cross ∂E_c , so these problems are indeed localized.

For the saturation equation, we upstream weight the convective terms $\gamma(s)$ so as to maintain stability. To do this, on a fine grid element E_f , we need to integrate by parts the term

$$\begin{aligned} \int_{E_f} \nabla \cdot (K \psi^n + \gamma(\mathbf{u}^n, s^n)) w dx \\ = \int_{\partial E_f} (K \psi^n + \gamma(\mathbf{u}^n, s^n)) \cdot \nu w ds. \end{aligned} \quad (8)$$

In order to balance capillary and gravitational forces, i.e., the terms $K \psi$ and $K \frac{\lambda_w(s) \lambda_n(s)}{\lambda(s)} (\rho_n - \rho_w) g \nabla z$ in γ , we have included the former term. This is necessary to properly balance the two terms on the discrete level, even when the problem is not convection dominated, since the balance of these forces is quite delicate. We also use a harmonically averaged permeability K on the interface. The result of separating scales on the discrete level follows.

Subgrid saturation equation: Wherein $w \in W_f = W_c \oplus \delta W$,

$$\begin{aligned} \int_{E_f} \phi \frac{s^n - s^{n-1}}{\Delta t} w dx \\ + \int_{\partial E_f} (K_H \psi^n + \gamma(\mathbf{u}^n, s_{\text{up}}^n)) \cdot \nu w ds \\ = \int_{E_f} f_w^n(s^n) w dx, \\ \int (\psi_c^n + \delta \psi^n) \cdot \delta \mathbf{v} dx = \int q(s^n) \nabla \cdot \delta \mathbf{v} dx, \end{aligned} \quad (9)$$

Coarse saturation equation:

$$\int (\psi_c^n + \delta \psi^n) \cdot \mathbf{v}_c dx = \int q(s^n) \nabla \cdot \mathbf{v}_c dx. \quad (10)$$

We linearize the saturation equation with Newton-Raphson, and solve for changes in s^n and ψ^n , given \mathbf{u}^n . Upstream weighting on the fine scale destroys the localization of the subgrid-scale problems posed over coarse element E_c . To circumvent this, we simply use the old Newton result for the upstream value when it traces out of E_c .

4 EFFICIENT SOLUTION

As stated above, the method is as hard to solve on the coarse scale as it is on the fine scale, since the coarse scales remain coupled to the subgrid scale. However, this coupling is relatively weak, and can be exploited through the use of numerical Greens functions. In this technique, on each E_c one solves a series of small problems.

The subgrid pressure equation (7) is linear, so it is the easier equation on which to describe the technique. The first problem to solve is given by omitting the coarse solution:

$$\begin{aligned} \int_{E_c} \nabla \cdot \delta \mathbf{u}_0^n \delta w dx &= \int_{E_c} f^n \delta w dx, \\ \int_{E_c} (\lambda(s^{n-1})K)^{-1} \delta \mathbf{u}_0^n \cdot \delta \mathbf{v} dx & \\ = \int_{E_c} \delta p_0^n \nabla \cdot \delta \mathbf{v} dx & \\ + \int_{E_c} \rho(s^{n-1}) \nabla z \cdot \delta \mathbf{v} dx. & \end{aligned} \quad (11)$$

Next we delete all the nonhomogeneous terms (terms not involving the solution p or \mathbf{u}). We then replace \mathbf{u}_c by a single finite element basis function and solve the resulting problem (one for each basis function, 8 in 2D and 18 in 3D). Let $\mathbf{v}_{c,j}$ be the j th such basis function. Then solve

$$\begin{aligned} \int_{E_c} \nabla \cdot \delta \mathbf{u}_j^n \delta w \, dx &= 0, \\ \int_{E_c} (\lambda(s^{n-1})K)^{-1} (\mathbf{v}_{c,j} + \delta \mathbf{u}_j^n) \cdot \delta \mathbf{v} \, dx & \quad (12) \\ &= \int_{E_c} \delta p_j^n \nabla \cdot \delta \mathbf{v} \, dx. \end{aligned}$$

Clearly if $\mathbf{u}_c = \sum_j \alpha_j \mathbf{v}_{c,j}$, then $\delta \mathbf{u} = \delta \mathbf{u}_0 + \sum_j \alpha_j \delta \mathbf{u}_j$ (and $\delta p = \delta p_0 + \sum_j \alpha_j \delta p_j$). This is our explicit representation of the subgrid-scale operator in terms of the coarse scale. It can be incorporated into the coarse scale equation (6) and solved for \mathbf{u}_c on the coarse grid. In this way, subgrid information is incorporated into the coarse scale without the need for pseudo-functions or averaged coefficients of any kind.

The saturation equation is similar, since it has been linearized by Newton-Raphson.

5 EXAMPLES

The logarithm of the random but correlated permeability field is depicted in Fig. 1. It varies from about 10 millidarcies to about 10 Darcies. Porosity is set uniformly to 25%. The domain is 80×10 meters, and the fine grid is 40×20 .

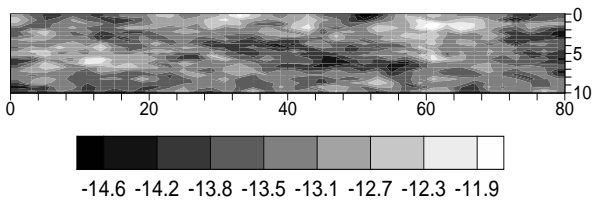


Figure 1. Base 10 logarithm of the permeability K (in m^2).

In the first example, we compute the initial pressure field of a 2D vertical petroleum waterflood problem, where the injection well is at the bottom right corner, and the extraction well is at the upper left. The initial saturation is in gravitational equilibrium. We show in Figure 2 the 40×20 full grid solution. This solution has 800 elements and requires 708 Jacobi preconditioned conjugate gradient iterations and 62 seconds of computer time.

The upscaled solution is shown in Figure 3. It uses a coarse grid of size 8×4 . This solution has 32 elements and requires 181 Jacobi preconditioned conjugate gradient iterations and 4 seconds of computer time. It is comparable to the fine solution; however, direct comparison is to be made with the coarse solution, since the upscaled and coarse solutions require about the same computing power. The coarse solution

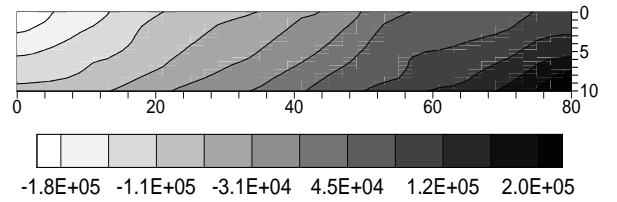


Figure 2. Fine scale (40×20) pressure contours of the vertical waterflood.

is shown in Figure 4. It takes 194 Jacobi preconditioned conjugate gradient iterations and also 4 seconds of computer time. The upscaling work is negligible.

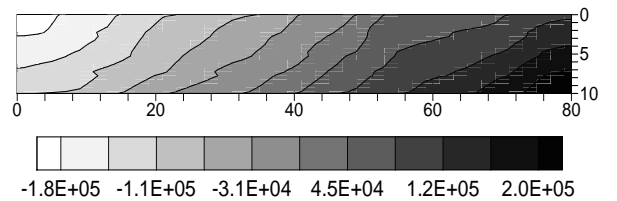


Figure 3. Upscaled (40×20 to 8×4) pressure contours of the vertical waterflood.

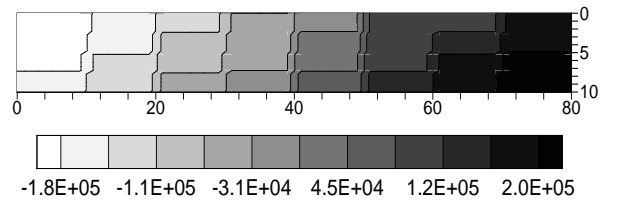


Figure 4. Coarse scale (8×4) pressure contours of the vertical waterflood.

In the second example, we solve a 2D horizontal waterflood. We use the same permeability field, but change the dimensions of the domain to 40×20 meters. The upscaled saturation at times 20 and 100 days are shown in Figures 5–6. As can be seen, fluid flows from coarse element to coarse element as expected. Previous results showed that the results were accurate when compared to the fine scale solution ((Arbogast 2000)); these results are clearly far superior to what one would expect from the 8×4 coarse grid solution (which is comparable in cost to the upscaling method).

It was discovered too late for this report that the saturation solution was not being computed correctly when the grid has a nonuniform aspect ratio. Since we have an 80×10 meter domain, the following results are tentative at best.

In the third example, we consider the 2D vertical downstream motion of the DNAPL. We let DNAPL be the wetting fluid, with density 1.2 and viscosity 4 times that of water. The background flow is 10 meters per year in the x -direction at the inlet face on the left, and 11 meters per year on the right. A constant contaminant source of 1 meter per year applies on the top face over the interval (10, 20) meters.

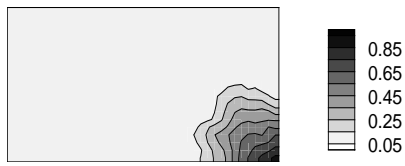


Figure 5. Upscaled (40×20 to 8×4) saturation contours of the horizontal waterflood.

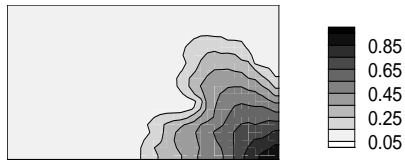


Figure 6. Upscaled (40×20 to 8×4) saturation contours of the horizontal waterflood.

We first solve the problem on a coarse mesh of size 8×4 . The DNAPL saturation at 100 days is shown in Figure 7. As can be seen, there is much more resolution than would be seen on a truly 8×4 mesh. However, it is also abundantly clear that spurious numerical artifacts are present. This is at least partly due to the aforementioned bug in the computer code. Some of the problem appears to be due to the fact that we use a fully finite element method without any mass lumping on the term

$$\int \psi^n \cdot \mathbf{v} dx$$

in (4b). This has the effect of making the inverse operator significantly nonpositive, so that nonmonotone solutions can arise.

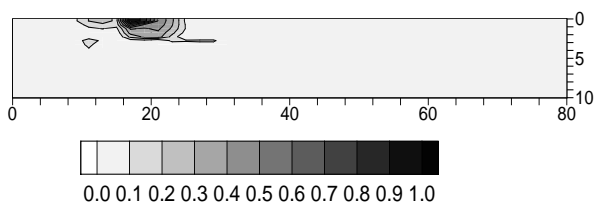


Figure 7. DNAPL saturation at 100 days with coarse mesh 8×4 .

Next we resolved the problem using mass lumping on the term

$$\int \delta \psi^n \cdot \delta \mathbf{v} dx$$

in (9b), by using the trapezoidal rule to approximate the integral. Unfortunately, this is not possible in (10) on the coarse scale, since higher order elements are used. In order to remove some of the numerical artifacts on the coarse scale, we do not decompose in the z-direction. That is, we take a coarse mesh of size 8×1 . The results appear in figures 7–9. The results are much improved.

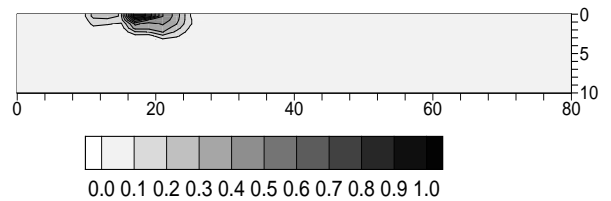


Figure 8. DNAPL saturation at 100 days with coarse mesh 8×1 .

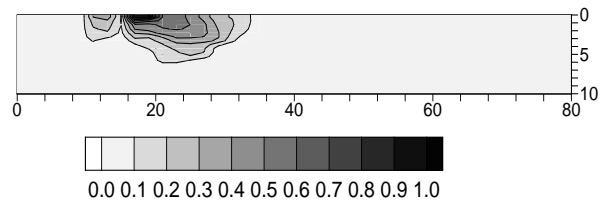


Figure 9. DNAPL saturation at 300 days with coarse mesh 8×1 .

6 CONCLUSIONS

The upscaling procedure does a good job on the pressure equation. It requires about the same time to compute as the coarse solution, but has drastically more resolution. The quality of the solution is comparable to the fine solution, even though the fine solution requires a great deal more computing power. The upscaling method can be used directly as a solution procedure. It could also be used as a preconditioner to the fine scale problem if one wants to solve it. In that sense, the procedure is like a one stage multigrid method.

The nonlinear saturation equation, in the absence of gravity, performs well (see also (Arbogast 2000)). At the moment, the code requires a uniform aspect ratio on the fine elements, due to some bug in the code. This is work in progress, and that bug will be corrected. No definitive statements can yet be made about the technique in the presence of gravity and near the residual saturations. Simulations with these features are much more delicate, and preliminary results available at press time for this report were difficult to assess. The mass lumping modification appears to be necessary, and to help considerably, but it does not naturally extend to the coarse scale. It is possible that perhaps the underlying treatment of the equations, rather than the upscaling technique itself, needs improvement to simulate the delicate nature of these flows near their residual values. Even if some of these difficulties cannot be resolved, the upscaling technique is clearly useful for the pressure equation, and it might still provide a good preconditioner to the fine scale saturation equation, since it has the ability to resolve fine scale features, and yet is considerably faster to compute than the full fine scale problem.

7 ACKNOWLEDGMENTS

This work was supported in part by the U.S. National Science Foundation under grants DMS-9707015 and SBR-9873326.

REFERENCES

- Arbogast, T. (1992). The existence of weak solutions to single-porosity and simple dual-porosity models of two-phase incompressible flow. *Journal of Nonlinear Analysis: Theory, Methods, and Applications* 19, 1009–1031.
- Arbogast, T. (2000). Numerical subgrid upscaling of two-phase flow in porous media. In Z. Chen, R. E. Ewing, & Z.-C. Shi (Eds.), *Multiphase flows and transport in porous media: State of the art*, Lecture Notes in Physics, pp. Submitted. Berlin: Springer.
- Arbogast, T., Minkoff, S. E., & Keenan, P. T. (1998). An operator-based approach to upscaling the pressure equation. In V. N. Burganos et al. (Eds.), *Computational Methods in Water Resources XII, Vol. 1: Computational Methods in Contamination and Remediation of Water Resources*, Southampton, U.K., pp. 405–412. Computational Mechanics Publications.
- Brezzi, F., Douglas, Jr., J., Duràn, R., & Fortin, M. (1987). Mixed finite elements for second order elliptic problems in three variables. *Numer. Math.* 51, 237–250.
- Brezzi, F., Douglas, Jr., J., & Marini, L. D. (1985). Two families of mixed elements for second order elliptic problems. *Numer. Math.* 88, 217–235.
- Chavent, G. & Jaffré, J. (1986). *Mathematical models and finite elements for reservoir simulation*. New York: Elsevier Science Publishers.
- Raviart, R. A. & Thomas, J. M. (1977). A mixed finite element method for 2nd order elliptic problems. In *Mathematical Aspects of the Finite Element Method*, Number 606 in Lecture Notes in Mathematics, pp. 292–315. New York: Springer-Verlag.